J. Fluid Mech. (1967), *vol.* 30, *part* 3, *pp.* 497–512
Printed in Great Britain

Nonlinear theory of open-channel steady flow past a solid surface of finite-wave-group shape

By M. S. HOWE
Imperial College, London

(Received 17 June 1967)

This paper deals with a detailed application of the Whitham theory of finite amplitude wave propagation to open-channel steady flow of water of infinite depth past a slowly modulated wavy wall. A numerical procedure first used by Garabedian & Lieberstein (1958) for the solution of 'stably-posed' elliptic Cauchy problems is employed to obtain a map of the wave pattern on the free surface of the water. The appearance of a 'shock' in this solution is discussed in terms of previous analytical and experimental results.

1. Introduction

A general theory governing the dispersion of slowly varying nonlinear wave trains has been proposed by Whitham (1965*a*, *b*). It consists in first supposing the wave train to be locally a uniform solution of the equations of motion from which an average Lagrangian is calculated in terms of the wave parameters. The equations describing the slow variation of these parameters are then derived by an application of Hamilton's Principle, that the time integral of the Lagrangian of the whole system is stationary.

Lighthill (1965, 1967) has considered in some detail applications of the theory to moderate amplitude waves on deep water (where certain 'pseudo-frequencies' are absent); he discusses in particular the dispersive effects of: (i) a large frequency spread, and (ii) substantial amplitude variation but almost constant wavenumber, on a finite amplitude wave-group. In his second paper a polynomial approximation to the average Lagrangian for deep water waves is derived, valid for all amplitudes. Whitham (1967) considers the one-dimensional propagation of finite amplitude waves in the case of finite depth. Both authors report substantial agreement between their analytical results and the results of Benjamin & Feir (1967) obtained in their experimental and analytical study of the instability of deep water waves.

A general account of the whole field was given in a recent Royal Society Discussion Meeting (Lighthill 1967). On page 33, there is a preliminary discussion of the application of the Whitham theory to waves that are stationary on a uniform stream. This is followed up in more detail in the present paper, which derives from an attempt to apply the Whitham theory to the ship-wave problem. Relative to a ship in uniform motion the wave pattern is stationary, and it should be

correspondingly easier to check theoretical predictions of nonlinear effects experimentally than in the non-steady problems previously considered.

The theory of ship-waves was first considered by Kelvin who showed that in general the wave pattern contains two families of waves: (i) the transverse waves which follow in the wake of the ship, and which tend to predominate at low Froude numbers, and (ii) the lateral or diverging wave system important at higher Froude numbers. On the whole more attention has been given to the transverse waves and it might be of more interest now to study the development of the lateral part of Kelvin's solution produced by a speedboat, say. Although a nonlinear treatment of waves generated by a ship moving at a high Froude number would be very valuable, it appears still too difficult to carry out in practice, and a somewhat simpler problem is treated here, chosen as a possible introduction to the ship-wave case. The difficulty in the latter case is that the energy of waves generated by a ship tends to be spread over a rather large region of wave-number space, so that near the ship it is in general impossible to have a gradually varying wave pattern. One cannot, therefore, specify suitably smooth boundary conditions such as are necessary if the theory is to predict the future development of the waves. An easier problem is to consider open-channel steady flow past a slowly modulated wavy wall of constant wavelength. In this case the energy induced in the wave motion occupies a relatively narrow band of wave-numbers.

This is the problem treated below. The water is assumed to have infinite depth so that a suitably modified form of Lighthill's formula for the average Lagrangian can be used. Although time dependence is now removed, the dispersion equation proves to be so complex that in the present context only a numerical solution can be contemplated.

2. Derivation of the dispersion equation

In terms of a Cartesian frame (x, y, z) with associated unit vectors $(\mathbf{i}, \mathbf{j}, \mathbf{k})$ the wall is given by $y = f(x)$, and in the undisturbed state the water will be supposed to occupy the region $-\infty < x < \infty, f(x) < y < \infty, -\infty < z < 0$. The mean velocity of the water is taken to be $U\mathbf{i}$.

Lighthill (1967) has given an approximation to the Lagrangian density function, $\mathscr{L}$, for waves on deep water in terms of the frequency ω and the wave-number κ. This says that $\mathscr{L}\kappa^2/\rho g$ (where ρ is the density of the water) is a function of $\Omega = \omega^2/g\kappa$ alone, and that the formula

$$\mathscr{L} = \frac{\rho g}{8\kappa^2}\{(\Omega-1)^2 - (\Omega-1)^3 - (\Omega-1)^4\} \tag{1}$$

holds to a good approximation throughout the interval from $\Omega = 1$ (infinitesimal amplitude waves) to $\Omega = 1{\cdot}20$ (waves of maximum height).

Equation (1) is written in terms of axes fixed relative to the undisturbed motion of the water. To obtain a form appropriate to steady flow at speed U past the wavy wall note that, if $\mathbf{v}$ is the phase velocity at a point where the wave-number is $\boldsymbol{\kappa} = (l, m)$, and the time frequency ω, then

$$\omega = \mathbf{v}.\boldsymbol{\kappa}.$$

In terms of the frame fixed relative to the wall the frequency is given by $(U\mathbf{i}+\mathbf{v}).\boldsymbol{\kappa}$, and if this vanishes then

$$\omega_1' = -Ul. \tag{2}$$

The required form of the Lagrangian is derived from (1) by replacing ω by $-Ul$ and the wave-number magnitude κ by $\sqrt{(l^2+m^2)}$.

To obtain the dispersion equation for the wave-field a phase function $\theta(x, y)$ is introduced by means of the definition

$$l = \theta_x, \quad m = \theta_y, \tag{3}$$

where suffixes denote partial differentiations. The level curves $\theta(x, y) =$ constant, map out the wave crests and troughs in the (x, y)-plane. The average Lagrangian $\mathscr{L}$ is now written in terms of the partial derivatives of θ and Hamilton's Principle applied in the simplified form

$$\delta \int\int \mathscr{L}(\theta_x, \theta_y)\, dx\, dy = 0.$$

The calculus of variations gives the Euler equation

$$\frac{\partial}{\partial x}\left(\frac{\partial \mathscr{L}}{\partial \theta_x}\right) + \frac{\partial}{\partial y}\left(\frac{\partial \mathscr{L}}{\partial \theta_y}\right) = 0,$$

or

$$\frac{\partial^2 \mathscr{L}}{\partial \theta_x^2}\theta_{xx} + 2\frac{\partial^2 \mathscr{L}}{\partial \theta_x \partial \theta_y}\theta_{xy} + \frac{\partial^2 \mathscr{L}}{\partial \theta_y^2}\theta_{yy} = 0; \tag{4}$$

this is a quasi-linear partial differential equation in θ, the coefficients depending only on the first derivatives θ_x and θ_y.

It is convenient to work in terms of dimensionless variables X, Y, L, M defined by

$$\left.\begin{aligned} X &= \frac{xg}{U^2}, \quad Y = \frac{yg}{U^2}, \\ L &= \frac{U^2 l}{g}, \quad M = \frac{U^2 m}{g}, \end{aligned}\right\} \tag{5}$$

in which case (4) takes the form

$$a(L, M)\theta_{XX} + 2b(L, M)\theta_{XY} + c(L, M)\theta_{YY} = 0, \tag{6}$$

where the coefficients are obtained from (1) to be:

$$\begin{aligned} a(L, M) = \{&(-2L^{10} - 10L^8M^2 + 24L^6M^2 - 56L^6M^4 + 6L^6 \\ &+ 10L^4M^2 - 24L^2M^6 + 2L^2M^4 - 2M^6) \\ &+ \sqrt{(L^2+M^2)}(-2L^6 - 15L^6M^2 + 9L^4M^2 + 90L^4M^4 + 9L^2M^4 - 2M^6)\}, \end{aligned} \tag{7}$$

$$\begin{aligned} b(L, M) = \{&(-16L^7M + 48L^7M^3 + 8L^5M + 16L^5M^3 + 16L^3M^3 + 32L^3M^5 + 8LM^5) \\ &+ \sqrt{(L^2+M^2)}(15L^7M - 9L^5M - 90L^5M^3 - 3L^3M^3 + 6LM^5)\}, \end{aligned} \tag{8}$$

$$\begin{aligned} c(L, M) = \{&(6L^{10} + 8L^8 - 42L^8M^2 - 2L^6 - 32L^6M^2 + 2L^4M^2 - 40L^4M^4 \\ &+ 10L^2M^4 + 6M^6) + \sqrt{(L^2+M^2)}(-15L^8 + 3L^6 + 90L^6M^2 - 9L^4M^2 - 12L^2M^4)\}. \end{aligned} \tag{9}$$

The boundary conditions determining the solution of the dispersion equation are such that L, M and θ are specified on some curve Γ in the (X, Y)-plane, and

it is important to know the form of (6) in the neighbourhood of this initial curve. This is governed by the sign of the discriminant

$$\Delta = b^2 - ac \tag{10}$$

the equation being elliptic if $\Delta < 0$, parabolic if $\Delta = 0$ and hyperbolic if $\Delta > 0$. In figure 1 the continuous curves are the loci of points for which Δ vanishes. The

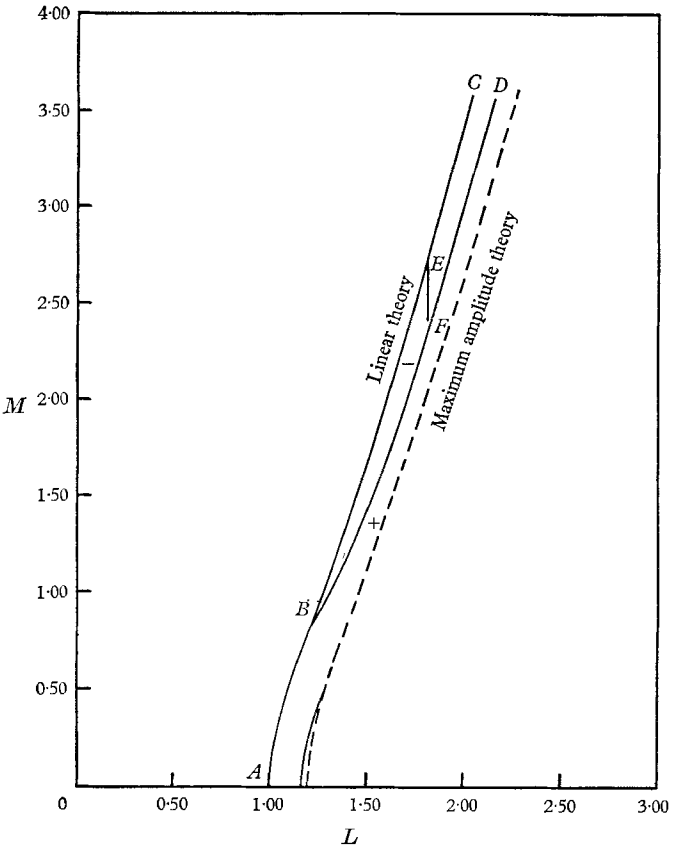

FIGURE 1. The mode of dispersion of a wave-group is determined by the spread of its energy in (L, M)-space between the linear theory and maximum amplitude theory curves. In the regions marked $-$, $+$ the dispersion is governed respectively by an elliptic equation and by a hyperbolic equation. The segment EF denotes the wave-number band occupied by the initial conditions used in the calculation.

magnitude of M is plotted against that of L, and on ABC they are related by the formula

$$L^2 = \sqrt{(L^2 + M^2)}, \tag{11}$$

which is that obtaining under the linear theory approximation. The portion BD separates the two regions marked $+$ and $-$ where respectively Δ is positive and negative. In the positive region the characteristics of the dispersion equation are real and distinct, and solutions θ would be expected to exhibit the characteristic splitting of the group velocity noted by Whitham (1965*a*). In the negative

area there are no real characteristics. Maximum amplitude waves are represented by the broken curve, which was shown by Lighthill (1967) to be given by

$$L^2 = 1{\cdot}20\sqrt{(L^2+M^2)}. \tag{12}$$

The region included between the linear theory curve and the maximum amplitude curve is that actually occupied by real waves.

The point B in figure 1 corresponds to $L = \sqrt{(3/2)}$, $M = \frac{1}{2}\sqrt{3}$, and its significance is illustrated by noting that, for example, on the linear theory of ship-waves, this is the point in wave-number space corresponding to the familiar cusp in the Kelvin wave pattern; the transverse waves occupy the segment AB and the lateral waves BC. Thus for moderate amplitude ship-waves the lateral waves are governed by an elliptic equation and the transverse waves by a hyperbolic equation. The present calculation is concerned with the lateral system, and replaces the ship by a wavy wall which results in the preferential generation of a wave pattern for which, near the wall, (L, M) lies well within the elliptic region.

3. The boundary conditions

The underlying idea of the Whitham theory is that the average Lagrangian is first calculated for a perfectly periodic wave-form which is afterwards allowed to vary slowly on a scale of wavelength. In an exactly parallel manner the boundary conditions for the present problem can be obtained by first supposing the wavy wall to have a constant amplitude. The case of a wave-group surface is then deduced by allowing the amplitude factor in the conditions so obtained to vary slowly on a scale of the wall wavelength.

Apart from requiring the slow variation of the wave parameters, the Whitham theory demands also that they be single-valued, or at least that, if two or more families of waves do overlap, the energy associated with one should completely swamp that of the others. Hence it is not feasible to attempt to obtain suitable boundary conditions too close to the wall. One must be content to prescribe the conditions near the wall, yet far enough away for spatial transients to be unimportant. In the case of the moderate amplitude cosine wall to be considered it will be seen that this can be satisfactorily achieved by taking the initial curve Γ to be the straight line $Y = 1$, parallel to the wall.

It is known (Lighthill 1967) that, for moderate amplitudes at least, the amplitude of a wave of given longitudinal wave-number L varies with distance Y from the wall as in the linear theory, although its position satisfies

$$\left(\frac{\partial X}{\partial Y}\right)_L = \left(\frac{\partial M}{\partial L}\right)_Y. \tag{13}$$

If Y is not larger than one or two wavelengths, substantial departures from the geometric optics approximation will not have occurred and energy will be received from the wall along the linear theory group velocity lines. These are given by

$$X - \chi(L)\,Y = \text{constant}, \tag{14}$$

where $\chi(L) = \partial M/\partial L$, and L and M are related by (11). Specifically, if the wall is given by

$$f(X) = A_0 \cos WX, \tag{15}$$

where A_0 and W are respectively the dimensionless amplitude and wave-number

of the wall, it will be shown that on a linear theory approximation the wave elevation ζ near the wall may be taken as

$$\zeta = \frac{-2A_0W}{\sqrt{(W^2-1)}} \sin[WX - WY\sqrt{(W^2-1)}]. \tag{16}$$

The factor $2A_0W/\sqrt{(W^2-1)}$ is the wave amplitude, and is assumed to be the first Fourier coefficient in the expansion of the waveform.

If A_0 is now allowed to vary slowly with X, $A_0 = A_0(X)$, near the wall the effect of this variation would be expected to be felt along the lines

$$X - \chi(W)Y = \text{constant}. \tag{17}$$

Thus on the initial line Γ, near enough to the wall for the accumulative effects of nonlinearity to be ignored, the appropriate wave amplitude would be

$$A = \frac{2WA_0(X-\chi(W)Y)}{\sqrt{(W^2-1)}}. \tag{18}$$

Here $A = \delta g/U^2$, where δ is the true amplitude.

To determine completely the wave-number (L, M) and phase θ on Γ for the real, finite amplitude waves, the compatibility relation connecting l, m and δ:

$$\omega^2 = g\kappa(1+\kappa^2\delta^2+\tfrac{5}{4}\kappa^4\delta^4+\ldots) \tag{19}$$

given by Lamb (1932, p. 420) must be used. As before $\omega^2 = U^2l^2$, $\kappa = \sqrt{(l^2+m^2)}$. The longitudinal wave-number L is taken to be W, that of the forcing mechanism, and the amplitude δ is given by (18). M is now computed from (19) by reverting the series and expanding M in terms of A and L. It is easily shown that

$$\begin{aligned} M &= M(L,A) \\ &= -L\sqrt{(L^2-1)}\left\{1-\left(\frac{L^2}{L^2-1}\right)(AL^2)^2+\left(\frac{L^2}{L^2-1}\right)\left(\frac{9}{4}-\frac{L^2}{2(L^2-1)}\right)(AL^2)^4+\ldots\right\}, \end{aligned} \tag{20}$$

where the minus sign anticipates backward-facing waves.

Hence, since (20) gives M as a slowly varying function of X, the boundary conditions for the dispersion equation can be set in the form,

$$L = W, \quad M = M(W,A), \quad \theta = LX + MY, \tag{21}$$

on $Y = 1$.

In the next section the linear theory solution will be obtained.

4. Linear theory solution

The wave pattern generated by a wall

$$Y = f(X), \tag{22}$$

where $f(X)$ is small, is analysed by introducing a potential $\phi(X, Y, Z)$ such that the dimensionless velocity $\mathbf{v}$ of the flow is given by

$$\mathbf{v} = \mathbf{i} + \nabla\phi. \tag{23}$$

On infinitesimal amplitude theory ϕ satisfies the equation

$$\frac{\partial^2\phi}{\partial X^2}+\frac{\partial^2\phi}{\partial Y^2}+\frac{\partial^2\phi}{\partial Z^2} = 0, \tag{24}$$

where $Z = zg/U^2$, in the region $-\infty < X < \infty$, $0 < Y < \infty$, $-\infty < Z < 0$. Apart from the usual condition at infinity, ϕ further satisfies

$$\frac{\partial \phi}{\partial Y} = \frac{df(X)}{dX}, \tag{25}$$

as $Y \to +0$, and

$$\left.\begin{aligned} \zeta + \frac{\partial \phi}{\partial X} &= 0, \\ \frac{\partial \phi}{\partial Z} - \frac{\partial \zeta}{\partial X} &= 0, \end{aligned}\right\} \tag{26}$$

or

$$\frac{\partial \phi}{\partial Z} + \frac{\partial^2 \phi}{\partial X^2} = 0, \tag{27}$$

at $Z = 0$, where $\zeta(X, Y)$ is the dimensionless surface elevation.

The problem is readily solved by considering the double Fourier transform $\psi(L, M; Z)$:

$$\psi(L, M; Z) = \frac{1}{\pi\sqrt{(2\pi)}} \int_{-\infty}^{\infty} dX \int_0^{\infty} \phi(X, Y, Z) \cos(MY) e^{-iLX}\, dY. \tag{28}$$

ψ is found to satisfy

$$\frac{\partial^2 \psi}{\partial Z^2} - (L^2 + M^2)\psi = \sqrt{\frac{2}{\pi}}\, iL\bar{f}(L), \tag{29}$$

where

$$\bar{f}(L) = \frac{1}{2\pi} \int_{-\infty}^{\infty} f(X)\, e^{-iLX}\, dX \tag{30}$$

and

$$\frac{\partial \psi}{\partial Z} = L^2 \psi, \tag{31}$$

as $Z \to -0$. The solution which is bounded as $Z \to -\infty$ is easily determined, and at $Z = 0$ reduces to

$$\psi = \sqrt{\frac{2}{\pi}}\, \frac{iL\bar{f}(L)}{[L^2 - \sqrt{(L^2 + M^2)}]\sqrt{(L^2 + M^2)}}. \tag{32}$$

The potential ϕ now follows from the inversion theorem for Fourier transforms, and at $Z = 0$ is,

$$\phi = \frac{2}{\pi} \int_{-\infty}^{\infty} dL \int_0^{\infty} \frac{iL\bar{f}(L)\, e^{iLX} \cos(MY)\, dM}{[L^2 - \sqrt{(L^2 + M^2)}]\sqrt{(L^2 + M^2)}}. \tag{33}$$

In evaluating this double integral account must be taken of the radiation condition that no waves enter or leave at $X = -\infty$. To do this consider the portion

$$\begin{aligned} I &= \int_0^{\infty} \frac{\cos(MY)\, dM}{[L^2 - \sqrt{(L^2 + M^2)}]\sqrt{(L^2 + M^2)}} \\ &= \frac{1}{2} \int_0^{\infty} \frac{e^{iMY} dM}{[L^2 - \sqrt{(L^2 + M^2)}]\sqrt{(L^2 + M^2)}} + \frac{1}{2} \int_0^{\infty} \frac{e^{iMY} dM}{[L^2 - \sqrt{(L^2 + M^2)}]\sqrt{(L^2 + M^2)}} \\ &= I_1 + I_2, \text{ say.} \end{aligned}$$

The radiation condition will be automatically satisfied if L is replaced by $L - i\epsilon$,

where ϵ is a small positive constant, I_1 and I_2 evaluated, and ϵ then allowed to tend to zero.

First note that both integrands possess simple poles at

$$M = \pm L\sqrt{(L^2-1)},$$

and branch points at $M = \pm iL$. To evaluate I_1 consider the integral about the contour shown in figure 2, consisting of the real axis from $M = 0$ to R, the circular

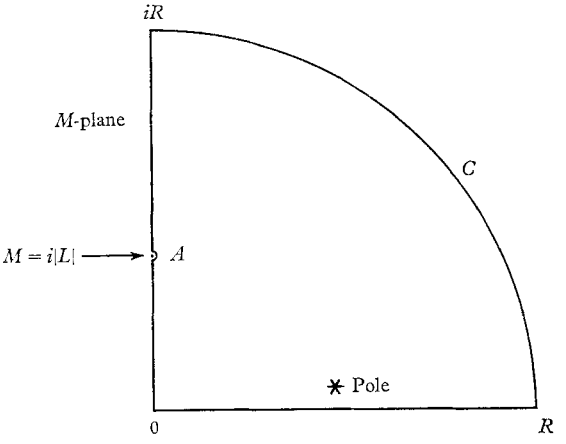

FIGURE 2. The contour used in evaluating I_1. The pole lies within the contour if $L < 0$ and outside if $L > 0$.

arc C from $M = R$ to iR, and the imaginary axis indented at the branch point A, from $M = iR$ to 0. When L is replaced by $L - i\epsilon$ in the integrand, the pole on the positive real axis is shifted into the interior of the contour if $L < 0$, and into the lower half-plane if $L > 0$. Hence, after letting $\epsilon \to 0$, its contribution to the integral may be written in the form

$$\frac{\pi i H(-L)}{L\sqrt{(L^2-1)}} \exp(-iLY\sqrt{(L^2-1)}) = H(-L)P(L), \text{ say},$$

where H is the Heaviside unit function. Thus, as $R \to \infty$,

$$I_1 = H(-L)P(L) + \int_0^A + \int_A^{i\infty},$$

i.e.
$$I_1 = H(-L)P(L) + \frac{1}{2}\int_0^{|L|} \frac{i\,e^{-\lambda Y}\,d\lambda}{[L^2 - \sqrt{(L^2-\lambda^2)}]\sqrt{(L^2-\lambda^2)}} + \frac{1}{2}\int_{|L|}^{\infty} \frac{e^{-\lambda Y}\,d\lambda}{[L^2 - i\sqrt{(\lambda^2-L^2)}]\sqrt{(\lambda^2-L^2)}}. \tag{34}$$

In a similar manner it is shown that,

$$I_2 = H(L)P(L) - \frac{1}{2}\int_0^{|L|} \frac{i\,e^{-\lambda Y}\,d\lambda}{[L^2 - \sqrt{(L^2-\lambda^2)}]\sqrt{(L^2-\lambda^2)}} + \frac{1}{2}\int_{|L|}^{\infty} \frac{e^{-\lambda Y}\,d\lambda}{[L^2 + i\sqrt{(\lambda^2-L^2)}]\sqrt{(\lambda^2-L^2)}}. \tag{35}$$

Combining I_1 and I_2 one eventually obtains

$$\phi = -2\int_{-\infty}^{\infty} \frac{\bar{f}(L)\exp\{iLX - iLY\sqrt{(L^2-1)}\}\,dL}{\sqrt{(L^2-1)}} + 2i\int_{-\infty}^{\infty} dL \int_{|L|}^{\infty} \frac{L^3\bar{f}(L)\,e^{-\lambda Y + iLX}\,d\lambda}{[L^4+(\lambda^2-L^2)]\sqrt{(\lambda^2-L^2)}} \tag{36}$$

at $Z = 0$.

In the first instance $f(X)$ is the uniform wall

$$f(X) = A_0 \cos(WX), \tag{37}$$

for which

$$\bar{f}(L) = \tfrac{1}{2}A_0[\delta(L+W)+\delta(L-W)], \tag{38}$$

where $\delta(x)$ is the Dirac function. Substitution in (36) and use of (26) leads to the expression

$$\zeta = \frac{-2A_0W}{\sqrt{(W^2-1)}}\sin(WX - WY\sqrt{(W^2-1)}) + \frac{2A_0W^4}{\pi}\int_W^{\infty} \frac{\cos(WX)\,e^{-\lambda Y}\,d\lambda}{[W^4+(\lambda^2-W^2)]\sqrt{(\lambda^2-W^2)}} \tag{39}$$

for the elevation of the free surface. The second term here represents a disturbance confined to the immediate neighbourhood of the wall, and the proportional error involved in its neglect is easily shown to be less than

$$\frac{\sqrt{(W^2-1)}e^{-WY}}{W\sqrt{(2\pi WY)}}.$$

Γ is taken to be the straight line $Y = 1$. The error along Γ is therefore less than 4 % and is rapidly decreasing further as the solution progresses (figure 4).

The dimensionless amplitude A thus takes the form anticipated in (18) on Γ, and since the group velocity lines are

$$X - \frac{(2W^2-1)Y}{\sqrt{(W^2-1)}} = \text{constant}, \tag{40}$$

the geometric optics approximation to the amplitude at (X, Y) finally takes the form

$$A = \frac{2W}{\sqrt{(W^2-1)}}A_0\left(X - Y\frac{(2W^2-1)}{\sqrt{(W^2-1)}}\right). \tag{41}$$

This is the value to be used in the conditions (21).

5. Solution of the dispersion equation

The problem of solving the dispersion equation,

$$a(L,M)\theta_{XX} + 2b(L,M)\theta_{XY} + c(L,M)\theta_{YY} = 0, \tag{42}$$

must now be considered. The solution is required in the half-plane $Y > 1$, and the boundary conditions to be imposed on $Y = 1$ have been shown to be

$$L = W, \quad M = M(W,A), \quad \theta = LX + MY, \tag{43}$$

where A is given by (41). Since (42) should be elliptic near the wall, W must be

chosen to lie in the elliptic region of wave-number space, and in the calculation presented below $W = 1{\cdot}8$. The values of L in the solution must be expected to be of the same order of magnitude, while, by (11), $M \sim 2{\cdot}7$. Under these circumstances it is difficult to construct an efficient approximation to the coefficients a, b, c which might enable some form of analytic solution to be obtained. It is more satisfactory to retain all the terms in the expressions for the coefficients and to adopt the numerical method of solution to be described.

The problem, then, is to solve the elliptic equation (42) under the Cauchy-type boundary conditions (43). In the classical sense this is 'incorrectly set'. However, the Hadamard concept of a well-posed initial value problem, namely that the solution be stable under arbitrary perturbations of the boundary conditions, is not applicable in this case. Here the boundary conditions are all functionally related, and arbitrary, independent perturbations therefore not permitted. Lieberstein (1959) has discussed such problems in relation to second order, linear elliptic equations. He defines the initial value problem to be 'stably-posed' if the perturbations can be confined to a restricted class of functions, S, for which the solution remains stable. It will be seen later that this definition may be extended to cover the present quasi-linear equation by requiring the class S, and so also the boundary conditions, to consist of those real functions for which there exists a sufficiently large region of the complex X-plane into which they may be analytically continued. This implies that the initial values of the wave parameters *and* their analytic continuations be smoothly varying functions.

Usually Cauchy-type boundary conditions are associated with hyperbolic equations, and the natural way is to solve by the method of characteristics. Recently techniques have been developed which permit elliptic type problems to be solved in the same way. Garabedian & Lieberstein (1958) have described in detail such a method, and used as an example the problem of subsonic flow behind a bow shock wave. A brief résumé will be given here.

Let (α, β) denote the characteristic co-ordinates of (42). When the equation is elliptic these will in general be complex. One can define a new pair of co-ordinates (ξ, η), however, by

$$\xi = \frac{\alpha+\beta}{2}, \quad \eta = \frac{\alpha-\beta}{2i}, \tag{44}$$

which have the property that real solutions of (42) in the (ξ, η)-plane correspond to real solutions in the (X, Y)-plane. Of course the relationship between (X, Y) and (ξ, η) is not known in advance, and must be calculated in a step-by-step manner simultaneously with L, M and θ.

In terms of these new co-ordinates the solution of the dispersion equation subject to the conditions (43) is equivalent to the solution of the canonical elliptic system

$$\begin{aligned}
X_\xi &= (bX_\eta - aY_\eta)/\sqrt{(ac-b^2)},\\
Y_\xi &= (cX_\eta - bY_\eta)/\sqrt{(ac-b^2)},\\
L_\xi &= (bL_\eta + cM_\eta)/\sqrt{(ac-b^2)},\\
M_\xi &= -(aL_\eta + bM_\eta)/\sqrt{(ac-b^2)},\\
\theta_\xi &= [(bL+cM)X_\eta - (aL+bM)Y_\eta]/\sqrt{(ac-b^2)},
\end{aligned}$$

under the same boundary conditions. This set of equations is conveniently denoted by

$$R_\xi = BR_\eta, \tag{45}$$

where R is the column vector of unknowns and B the matrix of coefficients. Since any function of a characteristic co-ordinate is still a characteristic co-ordinate, there is a freedom of choice of the initial curve γ in the (ξ, η)-plane along which the conditions (43) are to be imposed. This may be taken as the η-axis. Further, it may be supposed that along γ, $X = F(\eta)$, where F is an arbitrary real analytic function of η; in the present application $F(\eta) \equiv \eta$.

The important step now is to notice that, if (X, Y, L, M, θ) can all be considered as analytic functions of the *complex* variable $\eta = \lambda + i\sigma$, say, then, by the Cauchy–Riemann equations, the derivative R_η $(= R_\lambda)$ on the right-hand side of (45) may be replaced by R_σ/i. If λ is now held fixed at λ_0, the canonical system which is elliptic in the real (ξ, η)-plane becomes the hyperbolic system

$$R_\xi = (B/i)R_\sigma, \tag{46}$$

with the real characteristics

$$\xi \pm \sigma = \text{constant}$$

in the (ξ, σ)-plane. Hence, provided that for each λ_0 the data given on the (real) η-axis can be analytically continued into the complex η-plane to become data on the σ-axis, the hyperbolic system can be solved by a stable step-by-step procedure in the (ξ, σ)-plane. At $\sigma = 0$ the solution so obtained reduces to the solution in the real (ξ, η)-plane on the line $\eta = \lambda_0$. A complete covering of any portion of the real (ξ, η)-plane is obtained by repeating this procedure over a whole range of λ_0.

The philosophical difficulties involved in requiring that the data be continuable into the complex η-plane have already been discussed (Lighthill 1967). The Whitham theory assumes at the outset that the wave parameters are in some sense 'smooth' functions of position. It is now clear that their variation must be smooth enough to permit their being continued sufficiently far into the complex X-plane without meeting any singularities. This is precisely the case in the present problem.

The system (46) is solved numerically by adopting a finite difference approximation. That used here is the scheme originally proposed by Garabedian & Lieberstein in their paper. Let $\Delta\xi$, $\Delta\sigma$ denote positive increments in ξ and σ, and for a given λ_0 set

$$\left.\begin{aligned} R_{m,n} &= R[(\tfrac{1}{2}m\Delta\xi), (\tfrac{1}{2}n\Delta\sigma)], \\ B_{m,n} &= B[(\tfrac{1}{2}m\Delta\xi), (\tfrac{1}{2}n\Delta\sigma)], \end{aligned}\right\} \tag{47}$$

where $R(\xi, \sigma)$, $B(\xi, \sigma)$ are the vector and matrix of (46). The latter is now approximated by

$$R_{m+1,n} = R_{m-1,n} + s[(B_{m,n+1} + B_{m,n-1})/2i](R_{m,n+1} - R_{m,n-1}), \tag{48}$$

where $s = \Delta\xi/\Delta\sigma$. The characteristic roots of B/i are easily determined to be 1, -1, 0, so that the solution of the initial value problem for (48) would be expected to be stable provided $s \leqslant 1$. The truncation error in using (48) is of order $(\Delta\sigma)^2$.

It is convenient to take $\Delta\xi = \Delta\sigma$ and to adopt the mesh of points shown in figure 3, where only values of m and n whose sum is even are required. The only mesh points used in the calculation for which σ is negative occur at $n = -1$, and since both $R(\xi, 0)$, $B(\xi, 0)$ are real, their values at these points are given by the reflexion principle formulae:

$$R_{m,-1} = R^*_{m,1}, \quad B_{m,-1} = B^*_{m,1}, \tag{49}$$

where $R^*_{m,1}$, $B^*_{m,1}$ denote the complex conjugates of $R_{m,1}$, $B_{m,1}$.

The calculation may be summarized as follows.

I. Calculate $R_{0,n}$ for $n = 0, 2, 4, \ldots, 2N$, say, from the initial conditions.

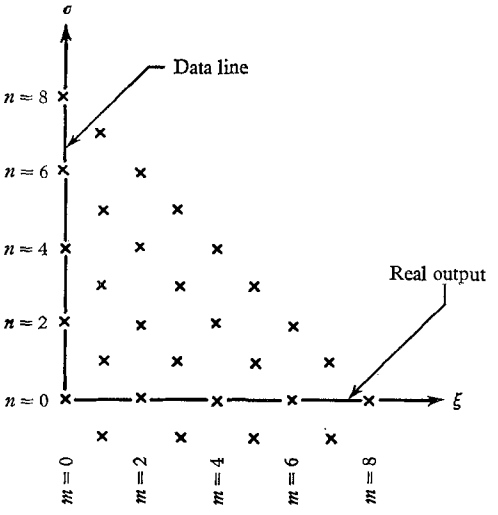

FIGURE 3. The system of mesh points used in the finite difference calculation. Complex data 'read-in' along the σ-axis produces real output along the ξ-axis.

II. Calculate $R_{1,n}$ for $n = 1, 3, 5, \ldots, 2N-1$, by means of (48) with $R_{-1,n}$ replaced by $\frac{1}{2}(R_{0,n+1} + R_{0,n-1})$ and s replaced by $\frac{1}{2}s$.

III. Calculate through repeated application of (48) the remaining values of $R_{m,n}$ such that $m+n$ is even and does not exceed $2N$.

The 'real output' of the calculation occurs along the ξ-axis in figure 3 at the N points $m = 2, 4, 6, \ldots, 2N$. This output will be the numerical value of the vector $R = (X, Y, L, M, \theta)$, so that each line $\eta = \lambda_0$ corresponds to a curve C, say, in the (X, Y)-plane along which L, M, θ take values given by the output R.

6. Numerical solution for the wavy wall

In the present calculation the slowly modulated wall is given by

$$f(X) = (S/W)\exp\{-(2X/L_G)^2\}\cos(WX), \tag{50}$$

where, relative to the length scale U^2/g, S/W is the maximum amplitude and L_G is the effective length of the wave-group surface. The wall is characterized by the

three dimensionless parameters S, L_G and W. S represents the maximum slope of the wall, L_G its length, and W the 'natural' frequency. The values used here are:

$$S = 0{\cdot}07, \quad L_G = 6\pi, \quad W = 1{\cdot}8.$$

The wavelength of the wall is $2\pi/1{\cdot}8 \sim 3{\cdot}5$, so that the wave-group surface consists effectively of seven humps, three on either side of the central maximum. The maximum slope is small, but reference to figure 1 shows that the region of wave-number space occupied by the initial conditions for this value of S is represented by the line EF, and the tip F of this line, corresponding to the maximum amplitude of the wall, is close to the boundary BD of the elliptic region. This would seem to indicate that quite large waves may be generated by moderate amplitude walls, and is a consequence of our considering the large Froude number case.

The object of the numerical calculation is to obtain a map of the curves of constant phase, θ, near the wall. This has been accomplished by solving the dispersion equation, in the manner described, above forty-one times at equally spaced points on the initial line $Y = 1$, from $X = -10$ to $X = +10$. In each case N, the number of output points was taken to be 30, and the mesh size $\Delta\xi = \Delta\sigma$ was never greater than 0·17. By interpolation between the output points on C, co-ordinates (X, Y) of the points of intersection of 100 level curves of θ with C (from $\theta = -21{\cdot}0$ to 18·6) were obtained, and the curves of constant phase subsequently plotted.

The calculation was performed on an IBM 7090 which requires about 3·7 min to obtain the output for each curve C, including the interpolation. The complete calculation requires a minimum of $2\frac{1}{2}$ h machine time. Except in the shock-like region to be discussed below the numerical procedure proved to be very stable, differences being noted only in the sixth significant figure on trebling the mesh size.

7. Discussion of results

The phase plot is shown in figure 4. It can be seen that the numerical calculation has produced a regular pattern of wave crests which on the left are almost rectilinear, but which tend to exhibit a bulging towards the left on moving in the positive X-direction. Eventually this bulging becomes so pronounced that a genuine discontinuity develops, resulting in the formation of a type of 'shock'. The dispersion equation remains elliptic except at the shock, where the numerical procedure becomes violently unstable. The interpretation of these results is that the wave amplitude is greatest where the bulging occurs. The latter is thus a consequence of amplitude dispersion, where larger amplitude waves have the larger phase velocity. Indeed, it is easy to see that the development and beginning of the shock occur approximately along that linear theory group velocity line which passes through the point marked P in the figure where the wall amplitude first becomes significant. Moreover, inspection of the numerical results reveals that below this line the wave-number lies further into the elliptic region than above, so that the waves here have a correspondingly larger amplitude. The

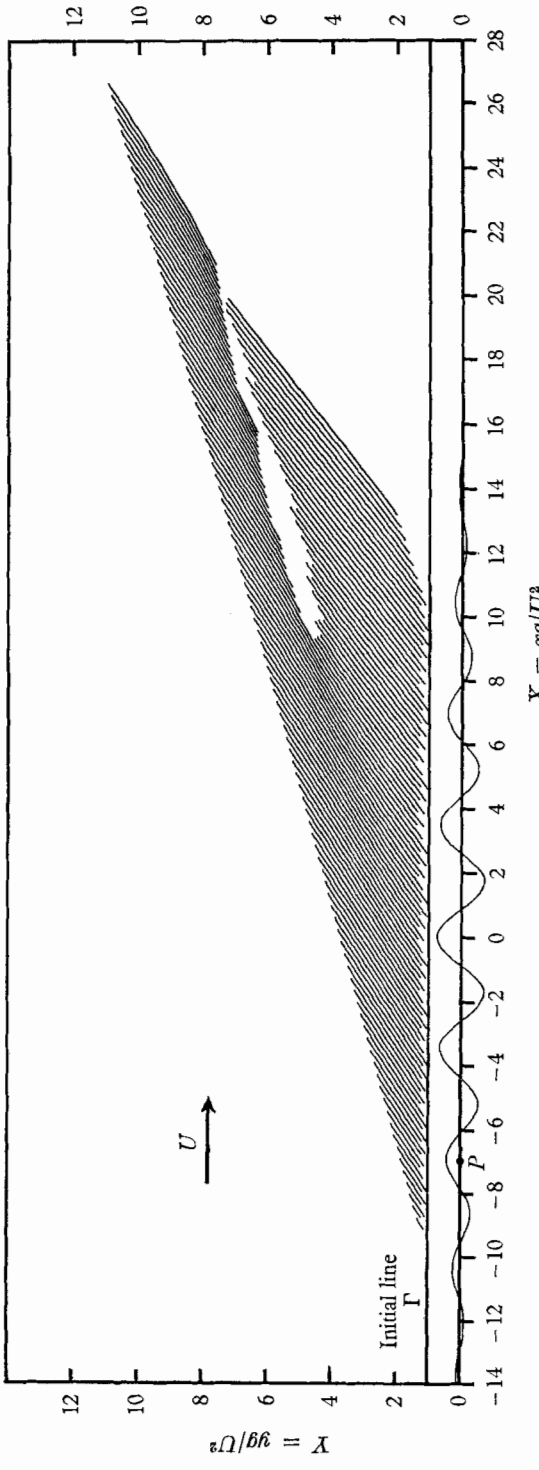

FIGURE 4. The wave pattern produced by flow past the wavy wall. The 'shock' develops approximately along the linear theory group velocity line from P. The wall is drawn to an exaggerated scale.

result is a tendency for the outer wave crests to lag behind because of their smaller phase velocities. This is clearly visible in the figure, and strikingly so after the shock has developed.

Across the shock there is an abrupt change in the direction of the wave crests and the magnitude of the wave-number, the waves being more closely packed on the side remote from the wall. Feir's experiments on one-dimensional, non-steady wave-trains indicate that in the region of the shock there is no pronounced turbulent dissipation or humping-up of the water: it is a confused region in which the wave crests execute a curious 'wiggle' and emerge on the other side changed in direction and spacing. It is possible, however, that the solution obtained here is not valid behind the shock. In the case of gas dynamics the simple wave approach to the solution behind a caustic gives misleading results for strong shocks, and the solution there must be derived from jump conditions across the shock.

Whitham (1965*a*) has suggested that it might be possible for shocks to develop in the hyperbolic case, and that they could probably be treated in the context of his theory by introducing suitable jump conditions. Lighthill (1965, 1967) has already anticipated the appearance of shocks in the elliptic case. In his treatment of the theory he studies the development of a slowly modulated wave-group of nearly constant wave-number, and predicts the appearance of a singularity in the wave-number and amplitude after a certain time, t_c, say. He shows further that there is an apparent 'incubation period' in which very little change in the wave-form occurs before time $t = 0{\cdot}7t_c$. This may be compared with the present case where the shock appears to develop quite rapidly from a fairly smooth wave pattern. Also, as in Lighthill's case, the wave-number magnitude is increased ahead of the shock and decreased behind.

Experimental support for the Whitham theory has so far been confined to the study of the development in time and distance of a one-dimensional wave group on deep water (Benjamin & Feir 1967), where a shock-like instability has been observed. Since this interesting phenomenon also occurs in the present case, where, moreover, the wave pattern is stationary, permitting relative ease of measurement, it seems desirable to do experiments with a wavy wall to see what happens in the neighbourhood of the discontinuity. Information obtained in this way would also be of considerable value to the further study of high Froude number ship-waves.

The author takes great pleasure in acknowledging his indebtedness to Prof. M. J. Lighthill, F.R.S., for his constant help and guidance throughout this investigation. He would also like to thank Dr C. I. Devanathan of the Indian Institute of Science, Bangalore, for many useful discussions concerning the material of this paper. Finally, the financial support of the Central Electricity Generating Board is gratefully acknowledged.

REFERENCES

BENJAMIN, T. B. & FEIR, J. E. 1967 *J. Fluid Mech.* **27**, 417.

GARABEDIAN, P. R. & LIEBERSTEIN, H. M. 1958 *J. Aero. Sci.* **25**, 109.

LAMB, H. 1932 *Hydrodynamics*, 6th ed. Cambridge University Press.

LIEBERSTEIN, H. M. 1959 *MRC Technical Summary Rept.* no. 81. Madison, Wisconsin.

LIGHTHILL, M. J. 1965 *J.I.M.A.* **1**, 269.

LIGHTHILL, M. J. (organiser) 1967 A Discussion on nonlinear theory of wave propagation in dispersive systems. *Proc. Roy. Soc.* A **299**, 1–145.

WHITHAM, G. B. 1965*a* *Proc. Roy. Soc.* A **283**, 238.

WHITHAM, G. B. 1965*b* *J. Fluid Mech.* **22**, 273.

WHITHAM, G. B. 1967 *J. Fluid Mech.* **27**, 399.